

# APPLICATION OF X-BAND LINACS

G. D'Auria

Sincrotrone Trieste, Trieste, Italy

## Abstract

Since the late 80's the development of Normal Conducting (NC) X-band technology for particle accelerators has made significant progress and has witnessed tremendous growth. The driving force behind this technological development, has been, and is, the interest of the scientific community in the construction of a Multi-TeV  $e^+e^-$  Linear Collider at a reasonable size and cost. The use of the X-band frequency allows for a much higher accelerating gradient per meter, when compared to the S and C bands. SLAC, with a major contribution from KEK, has been pioneering this development since the late 80's in the framework of the NLC/JLC projects. Later, in 2007, the same technology was chosen by CERN for CLIC, the 12 GHz Linear Collider based on the Two-Beam Acceleration (TBA) concept. In addition to these applications, X-band technology is also rapidly expanding in the field of X-ray FELs and other photon sources where it shows great potential. Here, a selection of X-band projects as well as the main applications of this technology at different international laboratories, is reported. The paper also includes a brief report on X-band medical and industrial applications.

## INTRODUCTION

In radar engineering the X-band is specified as frequencies in the range of 8-12 GHz. Already by the mid 60's, the SLAC "Blue Book" reported a clear interest for X-band technology in the process of selecting the best frequency for the SLAC Linac [1]. From the late 80's up to 2004, groups from SLAC, KEK, and later Fermilab, began a dedicated development of accelerating structures and components at 11.4 GHz (four times the frequency of the SLAC Linac), for a TeV-scale  $e^+e^-$  Linear Collider. A slowdown of these activities occurred in 2004, after the decision of the International Technology Review Panel (ITRP) to select L-band superconducting technology for the International Linear Collider (ILC). However, in 2007 CERN decided to lower the frequency of the Compact Linear Collider (CLIC) to 12 GHz (previously at 30 GHz), resulting in a renewed, and more vigorous, interest in X-band. Significant progress has been made in the last decade to raise the achievable accelerating gradients from the 65-70 MV/m declared at the end of the NLC/JLC program [2], up to the 100 MV/m reached on CLIC test structures [3], values far beyond those reached with the present S and C band technology. Today X-band developments are rapidly expanding due to their demonstrated potential in different segments of accelerator technology. X-band structures are currently used for very accurate beam diagnostics and e-bunch manipulations at many X-ray FEL facilities worldwide

[4,5,6]. Very ambitious projects using X-band Linacs, and based on Inverse Compton Scattering (ICS) for "extreme light" sources, are under construction or have been proposed [7,8]. Moreover, with the low bunch charge option currently considered for future X-ray FELs, X-band technology offers a low cost, compact solution for generating multi-GeV low emittance bunches. With the accelerating gradients mentioned above, an entire 1 GeV Linac can be easily housed in less than 20 m, representing a very cost effective solution for application with limited space [9].

## HIGH ENERGY COLLIDER

CERN's decision to lower the CLIC frequency to 12 GHz, has been a key factor in the revival of X-band work. The intense activity carried out in the framework of the CLIC international collaboration has led to important developments. At present the CLIC CDR has been completed [10] and the project is moving into the technical design of the main components. Concerning the high gradient X-band structures, two different modules, called T24 and TD24 (Dumped), have been successfully tested, with the CLIC RF pulse shape, to the CDR specifications of 100 MV/m (unloaded average gradient),  $\tau_{RF} > 170$  ns flat-top and a BDR/m  $< 3 \times 10^{-7}$ . Moreover, the measured RF breakdown rate (BDR) has shown good agreement with theory [11]. The baseline design of the CLIC structure, named TD26, has been completed and is very similar to TD24 [12]. The structure is designed for a  $2/3\pi$ , quasi-constant gradient, operating mode, with an average iris radius of 2.75 mm ( $r_{av}/\lambda_{rf}=0.11$ ). Four damping waveguides, with SiC absorbers, are integrated in each cell to provide for adequate HOM damping. Each structure is composed of 26 cells plus two couplers.

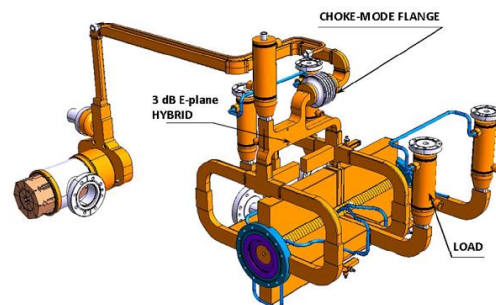


Figure 1: CLIC RF module

Two TD26, assembled together, make up what is called a "Superstructure" (SAS). Wakefield monitors, used for beam-based alignment, and accurate trajectory correction, are integrated into the first cell of every second structure of a SAS. To achieve the CLIC luminosity, the accelerating structures must be aligned to an accuracy of  $5 \mu\text{m}$  with respect to the beam. Figure 1 shows one CLIC

RF module, including its Power Extraction Transfer Structure (PETS), which extracts the RF power from the primary beam and transfers it to the main beam. The first TD26 structure is currently being fabricated and is expected to be ready for tests, in an RF module, early 2013. Other important tests planned for 2013 concern the effect of the beam loading on the RF breakdown rate, and a new wake field test to be performed at SLAC.

## X-RAY FELS AND PHOTON SOURCES APPLICATIONS

### Low charge X-ray FELs

Fourth generation light sources are based on FELs, driven by normal conducting (NC) or superconducting (SC) linacs. Soft and hard X-ray NC FEL facilities are presently operational (LCLS, SACLA, FERMI), in the construction phase (SwissFEL, PAL-XFEL, etc.), or are newly proposed in many international laboratories. While some use pre-existing S-band linacs, operating at 3 GHz (LCLS, FERMI), others (SACLA, PSI, PAL-FEL) use newer designs, based on the C-band technology, operating at 6 GHz. This choice increases the linac operating gradients, with an overall reduction of the machine length and cost. However, these advantages could be further enhanced using X-band linacs that can operate with gradients twice as high as the C-band linacs. The choice of the X-band is particularly advantageous for FEL operation using extremely short e-pulses ( $< 50 \mu\text{m}$ ) in the so called low charge regime (10-20 pC). These parameters guarantee very low wake field effects as well as reduced non-linear energy correlation along the bunch (no harmonic linearization needed). For example, a layout of a very compact hard X-ray FEL, with the same performance achieved by LCLS in low charge mode, driven by a 6 GeV X-band linac, has recently been studied at SLAC [13].

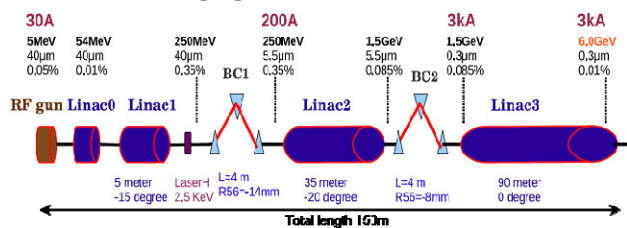


Figure 2: Layout of a 6 GeV X-band linac for a compact hard X-ray FEL

Beam simulations made with ASTRA and ELEGANT show that with two bunch compressors and a peak gradient of 80 MV/m (corresponding to an average gradient  $\leq 60$  MV/m), it is possible to produce 6 GeV e-pulses, with a length of 2-6 fs, 10 pC charge, and peak currents up to 3-4 kA. The slice energy spread and the normalized transverse emittance are less than 0.02% and 0.2 mm mrad respectively. No emittance dilution is observed for a 20  $\mu\text{m}$  rms, random offsets of the x-y structure axes. Figure 2 shows the proposed layout with a total linac length of 150 m. The study also considers an overall undulator chain of 30 m ( $\lambda_w=1.5\text{cm}$ ) to reach a

saturated power level above 10 GW. This performance is equivalent to the low charge mode of LCLS and is obtained in 180 m, as opposed to the 1230 meters of LCLS. Another study of an X-band linac for a soft ray X-FEL operating at a 1 KHz rep-rate, is discussed in [14].

### Extreme light sources based on ICS

Extremely bright, narrow bandwidth gamma ray sources, based on the Inverse Compton Scattering process (ICS) are attracting a growing interest among scientists for applications in what is called “Nuclear Photonics”, the study of nuclei with light. Gamma rays are the most energetic part of the EM spectrum and can penetrate through lead and other thick containers to detect the presence of nuclear weapons, radioactive waste, etc. Following the T-REX project at LLNL, that successfully demonstrated the feasibility of a Mono-Energetic Gamma-ray (MEGa-ray) source, ranging from 75 keV to 0.9 MeV, using a 120 MeV S-band linac [15], LLNL is currently assembling a new very compact source, VELOCIRAPTOR, to extend the production of radiation up to 2.5 MeV [16]. This new source is based entirely on a 250 MeV X-band linac. Figure 3 shows the layout of the machine under development at LLNL in collaboration with SLAC.

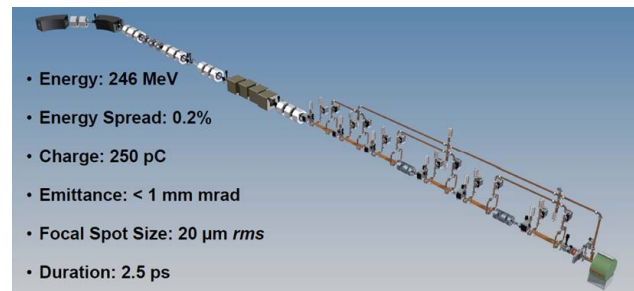


Figure 3: LLNL  $\gamma$ -ray source with expected performance

The electron source is a revised version of the first X-band photo-injector developed and tested at SLAC in 2003, Mark-0 [17]. The original design, tested up to 200 MV/m, has been improved with wider mode separations ( $>25$  MHz), a longer initial half cell, elliptical irises, and racetrack coupler, Mark-1. The main accelerator is composed of six SLAC T53 accelerating structures, developed and tested at SLAC at the beginning of 2000, in the framework of the NLC program. Although these structures have been operated up to 90 MV/m, with an acceptable BDR, for the LLNL project they will be operated at 70 MV/m, to keep an adequate margin. Two XL4 klystrons with an RF pulse compressor systems (SLED II) will provide the RF power for the entire machine. Operation is foreseen at 120 Hz, with 250 pC per pulse. LLNL is also assembling a X-band test station with a photo-injector, a single accelerating section, and beam diagnostics, to investigate accelerator optimization and future upgrades of the MEGa-ray technology. A very important (and challenging) issue for these sources is increasing the gamma-ray flux and the pulse repetition rate of the machine. Work is underway to investigate the photo-injector performance, with different cathode

materials (Cu and Mg) in multi-bunch mode, lowering the bunch charge to 25 pC and filling up to 1000 micro-pulses, at 11.4 GHz, in a macro-pulses train. The process must produce a significant increase in the average beam power while maintaining the beam brightness.

*X-band photo-injectors*

As part of a joint effort with LLNL, SLAC has recently started a dedicated R&D effort on X-band photo-injectors, with the assembly of the X-Band Test Area (XTA) in the NLCTA tunnel [18]. SLAC began their activity on X-band photo-injectors in the first years of 2000. The first photo-injector, installed at XTA has been Mark-0, that will provide operational experience before testing an improved version Mark-1, which is currently being fabricated at SLAC for XTA and LLNL, in the framework of the MEGA-ray program [19]. For the high gradients where they can operate (i.e. 200 MV/m), these photo-injectors produce very high brightness beams compared with the present S-band ones (i.e. a factor 3-4 over the LCLS injector). Figure 4 shows the Mark-0 gun and a plot of the energy gain of a 1.6 cell S-band gun operated at 115 MV/m, compared with a 5.5 cell X-band one operated at 200 MV/m. A  $\beta_{Lorentz}$  factor of 0.5 is reached after 3 mm at S-band and only at 1.2 mm at X-band.

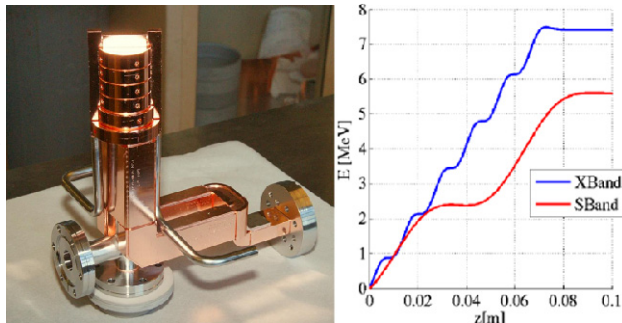


Figure 4: SLAC Mark-0 photo-injector and S-X band energy gain comparison.

Table 1 shows a comparison between the simulation results obtained running the XTA injector at 200 MV/m, with 250 and 20 pC, and results obtained with the same charge at LCLS at 115 MV/m.

Table 1: XTA and LCLS performance comparison

X-band			
Q (pC)	$\epsilon_{x,95\%}$ (mm mrad)	$\sigma_1$ (mm)	$B_p(Q/\sigma_1/\epsilon/1E3)$
250	0.28	0.184	4.85
20	0.075	0.109	2.44
LCLS			
Q (pC)	$\epsilon_{x,95\%}$ (mm mrad)	$\sigma_1$ (mm)	$B_p(Q/\sigma_1/\epsilon/1E3)$
250	0.40	0.620	1.01
20	0.15	0.220	0.61

Concerning the XTA activities and achievements, RF power tests started last March and the first photo-electrons were collected at the YAG screen, at the gun exit, in the end of July. At the beginning of August the beam was accelerated to 50 MeV with a 1 m (T105) accelerating structure.

R&D programs on X-band photo-injectors are also ongoing at UCLA, Particle Beam Physics Lab. (PBPL), in collaboration with INFN-LNF and ‘‘La Sapienza’’ University, in Rome. Two research lines are now in progress: the development of a hybrid photo-injector, a single accelerating unit made up of a Standing Wave (SW) gun and a Travelling Wave (TW) structure [20], and an asymmetric emittance photo-injector, for flat beams production [21]. Figure 5 shows the conceptual schematic of the hybrid photo-injector and the electric field on the axis.

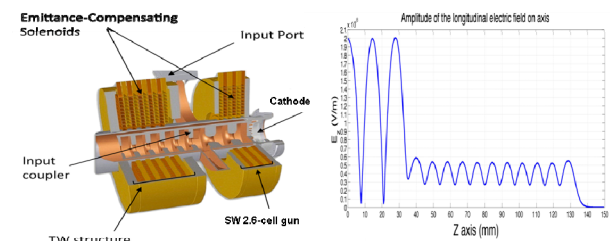


Figure 5: Hybrid photo-injector schematic with

The latest UCLA design for the hybrid photo-injector foresees a 2.6-cell SW gun followed by a 11-cell TW section (9 regular cells + input-output RF couplers). This structure strongly focuses the electrons in the longitudinal plane, acting as a velocity buncher. Two emittance compensating solenoids, with a peak field up to 6 kGauss on the SW gun and 2.5 kGauss on the TW structure, are foreseen. This novel design, more compact than a standard split system, exhibits a good RF matching and no circulator is needed on the main RF line. Table 2 summarizes the input and output parameters, obtained with numerical simulations, operating the gun at 200 MV/m. The extremely short pulse and low emittance obtained prove that these sources can reach a brightness higher than  $10^{16}$  (A/mrad<sup>2</sup>).

Table 2: Input/Output beam parameters

Input beam		Output beam @30 cm	
Charge	6.75 pC	Energy	4 MeV
Radius	67.5 $\mu$ m	Transv. size	58 $\mu$ m
Length	416 fs	Length	80 fs
$\epsilon_{Ter.}$	0.03 mm mrad	$\epsilon_{n,x,y}$	0.065 mm mrad
		$\Delta E/E$	0.60 %

The concept behind the asymmetric emittance photo-injector is based on a magnetized photo-cathode, which produces a beam already impressed with an angular momentum. The beam is then passed through a skew-quad triplet that splits the emittances. The project under development at UCLA employs a 9.3 GHz, 2.5-cell SW structure, operated at 200 MV/m, with 5.5 MW. Beam dynamics simulations show that with 1pC bunch charge, 1ps pulse length, and 25  $\mu$ m transverse beam size at the cathode, it is possible to have a 4.9 MeV beam, with a normalized transverse emittance of  $1.3 \times 10^{-7}$  mm mrad (circularly-magnetized) at the photo-injector exit. After the skew-quad array, ( $k_1, k_2, k_3 = -9.4, 6.0, 5.9$ , T/m), the emittances are splitted in  $\epsilon_{nx} = 2.6 \times 10^{-7}$  mm mrad and  $\epsilon_{ny} = 2.9 \times 10^{-9}$  mrad. The axial magnetic field at cathode is 6500 Gauss.

Copyright © 2012 by the respective authors — cc Creative Commons Attribution 3.0 (CC BY 3.0)

*Diagnostics and beam manipulation*

The Transverse Deflecting Cavity (TDC) is a diagnostic tool widely used at FEL linacs to measure the temporal profile and the slice properties of very short e-bunches [22]. The idea is to streak the e-bunches, using a RF structure operating in a properly polarized  $TM_{11}$  mode, and measure the beam profile on a screen downstream of the cavity. The diagnostics is further enhanced if the deflected beam is observed after an energy dispersion dipole, perpendicular to the RF deflection. The dispersion properties of the dipole allow each bunch slice to be measured, thus reconstructing the beam longitudinal phase space. Figure 6 shows the principle of operation of a TDC. With the beam energy and optics fixed, the measurement resolution depends on the TDC frequency and the gradient seen by the beam. The combined effect of these two parameters is that a X-band TDC can provide much higher resolutions (by a factor of 10) than a S-band one.

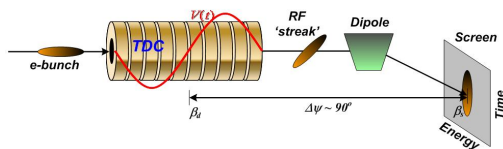


Figure 6: Operating principle of a TDC

A new application of this technique is now being implemented at LCLS for measuring the femtosecond temporal profile of the FEL photon beam [23]. An X-band deflecting system, made of 2 adjacent X-band sections, is being installed downstream the LCLS undulator for the continuous monitoring of all e-bunches. The two TDCs are positioned just before the beam dump and can be operated without interfering with the FEL users. The current design, at 13.6 GeV, is expect to achieve resolutions down to 2 fs, rms. The shot-to-shot slice analysis of each e-bunch, with FEL On and FEL Off, will indicate the parts of the beam that have radiated (losing energy), allowing a reconstruction of the current/photons time profiles. Figure 7 shows these reconstructed profiles [24].

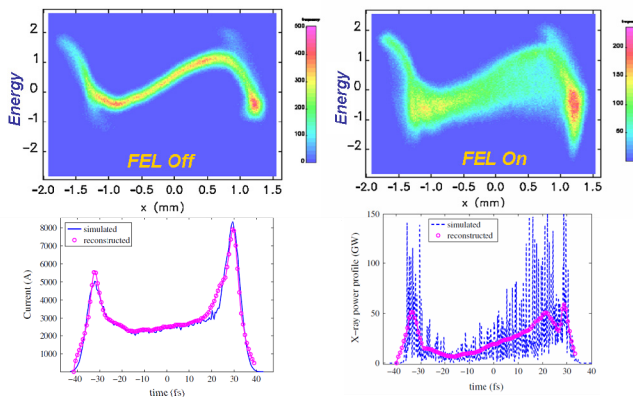


Figure 7: Reconstructed current profile and photon intensity with FEL Off (left) and FEL On (right).

Short X-band structures are also used for longitudinal phase space linearization at FEL linacs. They optimize the compression process, compensating for the second-order RF time-curvature and the second-order momentum

**01 Electron Accelerators and Applications**

**1A Electron Linac Projects**

compaction term,  $T_{566}$  at magnetic chicane. The first system, operating at 11.4 GHz, was installed and successfully commissioned at LCLS [25]. A second system recently came into operation at FERMI@Elettra FEL [26] and a third one is being installed at SwissFEL. The latter two are based on the same multipurpose 12 GHz accelerating structure developed in the framework of a collaboration between CERN, PSI and Sincrotrone Trieste [27]. The RF design, featuring 72 cells, 75 cm (active length),  $5/6\pi$  constant gradient, integrates two alignment monitors for accurate beam steering and trajectory correction. Moreover it is also possible to move the entire structure in the x-y plane by  $\pm 500 \mu\text{m}$ , with fine remote adjustments. The low energy part of FERMI linac is shown in Figure 8, with the X-band structure installed at roughly 180 MeV and the first bunch compressor (BC1) at 320 MeV.

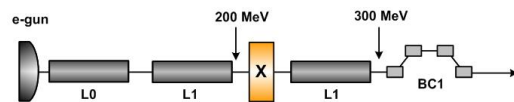


Figure 8: FERMI layout up to the first bunch compressor

The RF system is based on a 50 MW klystron (XL5), a 12 GHz scaled version of the SLAC XL4. The entire system has been installed in the last quarter of 2011 and commissioned up to June 2012. At present, for the nominal integrated gradient on the structure of 20 MV, it is operated at 50% of its nominal power. The measured RF phase and amplitude stabilities of 0.2 deg X-band and 0.05% rms are well in the specs. Tests have been carried out on the idle structure to verify the transverse wakes effects and the beam emittance degradation. Data, collected steering 350 pC, 6.5 ps (FWHM) beam  $\pm 1.0$  mm off-axes (x-y), did not show any particular emittance degradation if the beam stays aligned on the axes within one hundred microns.

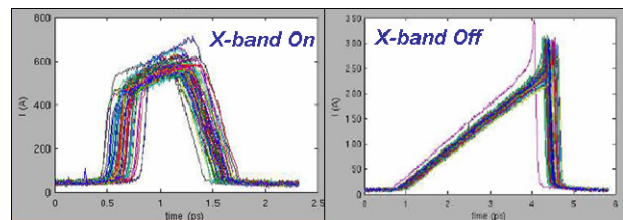


Figure 9: Current temporal profiles at BC1

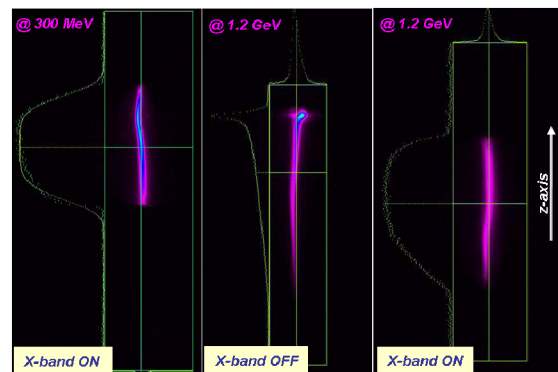


Figure 10: Bunch charge distribution at linac exit

Beam tests, performed at different cavity set-ups (17-20 MV) and compression factors (5-10) provided very good results. Figures 9-10 show the current temporal profile downstream BC1, and the bunch charge distributions at linac exit, with X-band On/Off, taken with two TDCs at 300 MeV and 1.2 GeV, on 150 e-pulses (15 sec).

For the tests, the machine was operated with only one bunch compressor. The flat-topping effect induced by the X-band in the two distributions is evident, with a net increase of the peak current (up to 600 A), and a very positive impact of the on the FEL performance.

## INDUSTRIAL AND MEDICAL APPLICATIONS

In the last decade, the industrial and medical applications of X-band linacs have experienced significant growth. The advantages in using higher frequencies with respect to the most widely used S-band technology, came from its compactness, reduced weight and ease in handling and control. At X-band, the higher structure shunt impedance allows for higher efficiency in RF power conversion at a given beam energy. Moreover the breakdown voltages are much higher and filling time shorter. Most of the industrial and medical X-band linacs, cover the 1-10 MeV energy range and are operated at 9.2-9.4 GHz, using 1-2 MW pulsed magnetrons, at up to 0.1% duty cycle. A high power pulsed klystron (5 MW-20 kW) is also available at 9.3 GHz, but the offer at higher frequency is very limited. Portability makes X-band widely used for on-site inspections, i.e. bridges, chemical plants, pipe lines [28] and non-destructive analysis, i.e. cargo screening, food processing, etc. Novel compact inexpensive linacs, 1-2 MeV/10-100  $\mu$ A average current, are also being developed for replacement of radionuclides sources, used for industrial radiography, Ir-192, Cs-137, Co-60 [29]. Medical applications greatly benefit from X-band for the reduced size of the beams and the possibility to easily have “self-shielded machines”, minimizing stray radiation and leakages in treatment rooms. The most common applications that use X-band linacs are the Intra-Operative Radiation Therapy (IORT), where the electron beam radiation is directly delivered during surgery, and Stereotactic Radiosurgery, that uses an image-guided system to precisely deliver intensity modulated radiation to the focal lesion. For their compactness, X-band linacs are also being considered for Hadrontherapy, where it would be desirable to have “single room facilities” in which a proton linac rotates around the patient [30].

## CONCLUSION

Applications of X-band technology in linacs is rapidly expanding due to its great potential already shown in different areas of particle accelerators. Recent results, concerning the accelerating gradients obtained at CLIC, demonstrate the feasibility of 100 MV/m operation with NC accelerating structures at 12 GHz. This will also benefit the interest for very compact linacs for X-ray FELs. The developments of very high brightness X-band photo-injectors are very promising and the use of X-band

structures for diagnostics and beam manipulation at FEL linacs is continuously evolving. Very challenging R&D programs with X-band linacs have been undertaken in laboratories pursuing high intensity gamma sources, to increase the average power of the machines with multibunch operations.

Moreover, the great attention shown in the last two years by the scientific community for the use of X-band technology has also stimulated the interest in industry for the production of high power RF components. Two 50 MW, 12 GHz klystrons are currently at an advanced stage of manufacturing at industry.

## ACKNOWLEDGEMENTS

The author is very grateful to U. Amaldi, S. Döbert, A. Degiovanni, J. Kovermann, G. McMonagle, I. Syratchev, W. Wuensch (CERN); C. Adolphsen, C. Limborg, P. Krejcik, T. Raubenheimer, S. Tantawi, A. Vlieds (SLAC); C. Barty, R. Marsh (LLNL); J. Rosenzweig, A. Valloni (UCLA); B. Spataro (INFN-LNF); M. Uesaka (University of Tokyo); E. Tanabe (AET Inc.); A. Tafo (Accuray); F. Manelli (Elekta) for providing informations about their activities and R&D programs on the X-band. Furthermore, the colleagues of the Linac group and FERMI commissioning team are acknowledged.

## REFERENCES

- [1] R.B. Neal “The SLAC Two Mile Accelerator”, W.A. Benjamin, 1968.
- [2] C. Adolphsen, SLAC-Pub 11224 (2005).
- [3] W. Wuensch, HG2012 Workshop, 18-20 April 2012, KEK, Tsukuba, Japan.
- [4] P. Emma, LCLS-TN-01-1, (2001).
- [5] G. D’Auria et al., IPAC’10, Kyoto, Japan, TUPE015.
- [6] J.W. Wang et al., SLAC-Pub 13444 (2008).
- [7] F.V. Hartemann, LINAC’10, Tsukuba, Japan MOP005.
- [8] ELI-NP, Magurele, Romania, <http://www.eli-np.ro/>
- [9] G. D’Auria, NIM A 657 (2011).
- [10] <http://clic-study.org/accelerator/CLIC-ConceptDesignRep.php>
- [11] A. Grudiev et al., PRST 12, 102001 (2009).
- [12] A. Grudiev et al., LINAC’10, Tsukuba, Japan, MOP068.
- [13] Y. Sun et al., PRST 15, 030703 (2012).
- [14] R. Walker et al., FEL’11, Shanghai, Cina, TUPB18.
- [15] D. Gibson et al., PRST 13, 070703 (2010).
- [16] S. Anderson et al., NIM A 657 (2011).
- [17] A. Vlieds et al., AIP Conf. Proc. 691, June 2003.
- [18] C. Limborg et al., PAC’11, New York, USA, MOP015.
- [19] A. Vlieds et al., IPAC’12, New Orleans, LA, USA, WEPPB007.
- [20] J. Rosenzweig et al., NIM A 657 (2011).
- [21] A. Valloni et al., AAC’12, Austin, Texas, USA.
- [22] P. Emma et al., LCLS-TN-00-12, (2000).
- [23] P. Krejcik et al., BIW’12, Newport News, VA, USA.
- [24] Y. Ding et al., PRST 14, 120701 (2011).
- [25] P. McIntosh et al., SLAC-Pub 11270.
- [26] G. D’Auria et al., IPAC’12, New Orleans, LA, USA, TUPPP054.
- [27] M. Dehler et al., IPAC’12, New Orleans, USA, MOOBC03.
- [28] M. Uesaka et al., NIM A 657 (2011).
- [29] S. Boucher et al., IPAC’12, New Orleans, LA, USA, THPPR069.
- [30] U. Amaldi et al., RAST Vol. 2 (2009) 111–131.